International Journal of Recent Development in Engineering and Technology
Website: www.ijrdet.com (ISSN 2347 - 6435 (Online)) Volume 2, Issue 2, February 2014)

SEISMIC GABOR DECONVOLUTION AND THE COLOR CORRECTION TO WHITE-REFLECTIVITY ASSUMPTION

M.S Saravanan[1], Dr Hesham Abu Haleemah[2], P.K Kumaresan[3]

[1]*Associate Professor, Dept of Civil Engineering, Annapoorana Engineering College, Salem, ermss64@gmail.com*
[2]*Associate Professor, Jazan University ,KSA abouhahimah58@yahoo.com*
[3]*Professor, VMKV Engineering College, Peria Seeragapadi, Salem 636 308,pkkumaresan@rediffmail.com*

***Abstract*— Deconvolution is an essential part of seismic data processing. The deconvolution algorithm is derived from the corresponding convolution model. Conventional deconvolution methods are developed based on the stationary convolution model, such as Wiener spiking deconvolution. However, the seismic trace is nonstationary due to attenuation during the propagation for various reasons such as attenuation and geometric spreading. Deconvolution algorithms usually assume that the reflectivity is a random series, meaning that reflectivity has a white amplitude spectrum. In practice, the reflectivity is colored, i.e., the magnitude of its Fourier amplitude spectrum demonstrates obvious frequency dependency. The white reflectivity assumption can lead to distortion of reflectivity estimation. The nonstationary characteristic of both seismic trace and true reflectivity can be corrected in a nonstationary way. This chapter gives a basic introduction to Gabor deconvolution, and presents the color correction method to white-reflectivity assumption for Gabor deconvolution. The influence of the time-variant reflectivity color is analyzed in detail, and synthetic data and field data are used to evaluate the color correction method.**

***Keywords*— Dconvolution, Gabor, seismic trace.**

1. GABOR DECONVOLUTION

1.1 The Gabor transforms

Gabor transform (GT) provides a manner of time-frequency decomposition of a signal. In this section, we will follow Margrave and Lamoureux (2001), Margrave et al (2011) to give a brief introduction to the GT. The continuous GT of a signal can be defined as (Mertins, 1999)

$$S_G(\tau, f) = \int_{-\infty}^{\infty} s(t)\vartheta(t-\tau)e^{-j2\pi ft}\,dt \quad (1.1)$$

where the Gabor analysis window, and denotes the center of the analysis window. We can see that the continuous GT gives local spectrum of the signal by weighting the signal with a window function before the Fourier transform.

By sliding the analysis window along the signal, GT produces a collection of local spectra. So, a time-frequency decomposition of the signal is obtained. Even if signal is nonstationary for the whole time range, can still be regarded to be approximately stationary within a specified time window. From this point of view, GT can give a better characterization of nonstationary signal compared with Fourier transform. Given, the signal can be reconstructed as

$$s(t) = \iint_{-\infty}^{\infty} S_G(\tau, f)\,\gamma(t-\tau)e^{-j2\pi ft}\,df\,d\tau \quad (1.2)$$

where is the Gabor synthesis window. To achieve a perfect reconstruction, the analysis window and synthesis window should satisfy the following condition

$$\int_{-\infty}^{\infty} \gamma(t)\vartheta(t)\,dt = 1 \quad (1.3)$$

When and , Gabor transform reduces to Fourier transform. So, Fourier transform can be viewed as a particular case of Gabor transform. For practical implementation, a discrete form of Gabor transform should be employed. Given a time spacing of and frequency spacing of , the discrete Gabor transform is given by

$$S_G(m,n) = \int_{-\infty}^{\infty} s(t)\vartheta_{m,n}(t)\,dt, \quad (1.1)$$

where is the Gabor frame defined as

$$\vartheta_{m,n}(t) = \vartheta(t - m\Delta\tau)e^{-i2\pi n\Delta f} \quad (1.5)$$

If the Gabor frames are orthonormal to each other, the signal can be recovered from the Gabor frame operator defined by

$$V_G(s(t)) = \sum_{m,n\in Z} S_G(m,n)\,\vartheta_{m,n}(t). \quad (1.6)$$

International Journal of Recent Development in Engineering and Technology
Website: www.ijrdet.com (ISSN 2347 - 6435 (Online)) Volume 2, Issue 2, February 2014)

However, the Gabor frames in equation (1.5) do not form an orthonormal basis. For the DGT, the reconstruction of signal should involve the inversion of the Gabor frame operator. So, the recovery of can be formulated as

$$s(t) = \sum_{m,n\in Z} S_G(m,n)\, V_G^{-1}\vartheta_{m,n}(t) = \sum_{m,n\in Z} S_G(m,n)\gamma_{m,n}(t)$$, (1.7)

where is the dual Gabor frame. The Gabor frames are complete in on condition that (Margrave and Lamoureux, 2001). We can exactly recover the signal by (1.7). However, it is hard to get an inversion of the Gabor frame. In practice, we can choose an approximate way to implement the discrete Gabor transform.

$$\vartheta(t-k\Delta\tau) = \frac{\Delta\tau}{\delta\sqrt{\pi}} e^{-[t-k\Delta\tau]^2\delta^{-2}}$$, (1.13) where is the Gaussian half-width. Margrave and Lamoureux (2001) gave a precise expression of the summation of the Gaussians, which is

$$\sum^{k\in S} \vartheta(t-k\nabla t) = 1 + 2\cos\left(\frac{\nabla t}{\delta\pi}\right)\vartheta_{-[\pi\perp\setminus\nabla t]_3} + \cdots$$ (1.11) We can use the second term in (1.14) to estimate the approximate errors. So, the error can be made as small as we want by increasing the ratio . For geophysical applications, the error is negligible when (Margrave and Lamoureux, 2001).

The inherent end effect of the approximate discrete Gabor transform can be further reduced by normalization using the summation curve. The Gabor transform given in equation (1.10) can be normalized as (Margrave and Lamoureux, 2001)

$$\hat{s}_k(f) = \frac{\int_{-\infty}^{\infty} s_k(t) e^{-j2\pi f t} dt}{h(k\Delta\tau)}$$, (1.15) Where is the actual summation curve of Gabor transform.

I.

II. The Gabor deconvolution algorithm

Gabor deconvolution is based on a nonstatioanry convolution model of the seismic trace. Margrave and Lamoureux (2002) presented a seismic trace model addressing the seismic wavelet and the nonstationary effect of constant- attenuation. The nonstationary convolution model is introduced in chapter 1, and will be restated here for introducing Gabor deconvolution algorithm. The attenuated seismic trace can be modeled as

$$s(t) = M(t)\int_{-\infty}^{\infty} \alpha_Q(\tau,t) r(\tau) e^{-j2\pi f t} dt$$, (1.16)

where and are the Fourier spectra of the seismic trace and seismic source wavelet respectively; is the reflectivity, and is the constant- transfer function given by

$$\alpha_Q(\tau,f) = e^{-\frac{\pi f\tau}{Q} + jH(\frac{\pi f\tau}{Q})}$$, (1.17) where denotes the Hilbert transform. Then, the Gabor transform of the attenuated seismic trace can be approximated by (Margrave and Lamoureux, 2002; Margrave et al, 2011)

$$S_G(\tau,f) \approx W(f)\alpha_Q(\tau,f)R_G(\tau,f)$$, (1.18) with an assumption thatwith a 2-D boxcar over where is the Gabor transform of reflectivity. Based on equation (4.18), can be estimated by smoothing. The simplest smoothing can be achieved by convolving . Let be a proper smoothing of Q . With a minimum-phase assumption, the attenuated wavelet or propagating wavelet is estimated as

$$W(f)\alpha_Q(\tau,f) \approx \overline{|S_G(\tau,f)|} e^{j\varphi(\tau,f)}$$, (1.19) where the Hilbert gives the phase transform (over frequency),

$$\varphi(\tau,f) = H(ln\overline{|S_G(\tau,f)|})$$. (1.20) Therefore, an estimation of the reflectivity can be formulated in the Gabor spectral domain as

$$R_G(\tau,f)_{est} = S_G(\tau,f)\mathrm{D}(\tau,f),$$ (1.21) where is the deconvolution operator formulated as

$$\mathrm{D}(\tau,f) = \frac{1}{\overline{|S_G(\tau,f)|} + \mu A_{max}} e^{-j\varphi(\tau,f)}$$, (1.22) in which is the stability factor, and is the maximum value of $\overline{|S_G(\tau,f)|}$. The magnitude of the Gabor spectrum of attenuated seismic trace is shown in Figure 4.8. We can see the amplitude decays with increasing frequency and travel-time. The magnitude of the Gabor spectra for the two-deconvolution algorithms is shown in Figure 4.9 and 4.10.

International Journal of Recent Development in Engineering and Technology
Website: www.ijrdet.com (ISSN 2347 - 6435 (Online)) Volume 2, Issue 2, February 2014)

For the stationary deconvolution, the Gabor spectrum of the estimated reflectivity is obviously distorted compared to the one shown in Figure 4.7. For the Gabor deconvolution, the Gabor spectrum of the estimated result has magnitude of approximately the same level over all frequency (within the given frequency band) and travel time.

III. Conventional Gabor deconvolution.

When this assumption violated, the estimated result might be distorted as well.

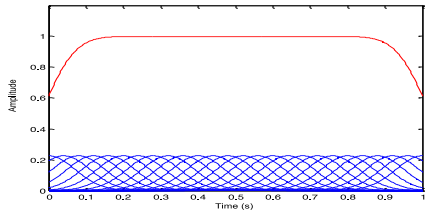

Figure 4.1. The summation curve of a set of Gaussian windows with half-with of $\delta = 0.1s$ and spacing of $\Delta\tau = 0.04s$ (red: summation curve; blue: Gaussian windows).

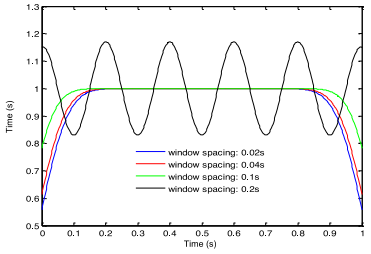

Figure 4.2. The summation curves of a set of Gaussian windows with fix Gaussian width of $0.1s$ and varied window spacing of $0.02s$, $0.04s$, $0.1s$, and $0.2s$.

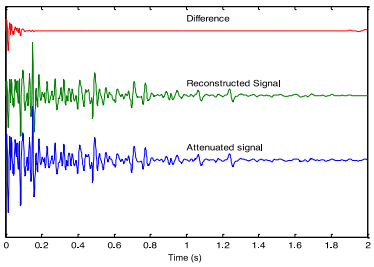

Figure 4.3. Signal reconstruction using approximate discrete Gabor transform.

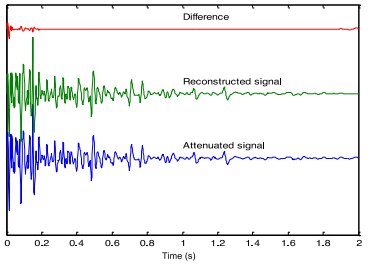

Figure 4.4. Signal reconstruction using normalized discrete Gabor transform.

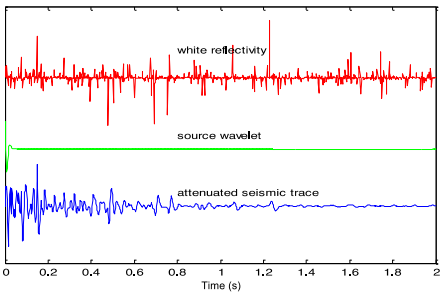

Figure 4.5. An attenuated seismic trace created from random/white reflectivity by a constant-Q model. The source wavelet is a minimum-phase wave with a dominant frequency of $40Hz$ and the Q value is 50.

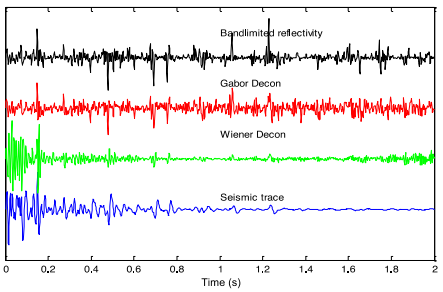

Figure 4.6. Results of the Gabor deconvolution and Wiener spiking deconvolution. (blue) The attenuated seismic trace shown in Figure 4.5. (green) The result of Winner spiking deconvolution proceeded by AGC. (red) The result of Gabor deconvolution without proceeding gain correction. (black) The bandlimited actual reflectivity.

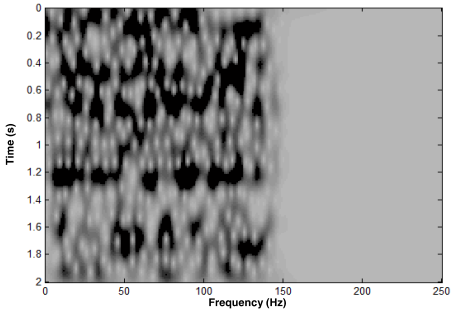

Figure 4.7. Magnitude of the Gabor transform of the band-limited actual reflectivity in Figure 4.6.

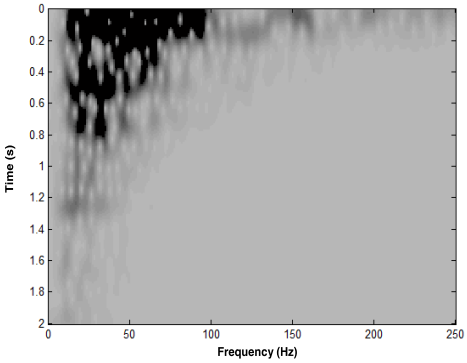

Figure 4.8. Magnitude of the Gabor transform of the attenuated seismic trace in Figure 4.6.

International Journal of Recent Development in Engineering and Technology
Website: www.ijrdet.com (ISSN 2347 - 6435 (Online)) Volume 2, Issue 2, February 2014)

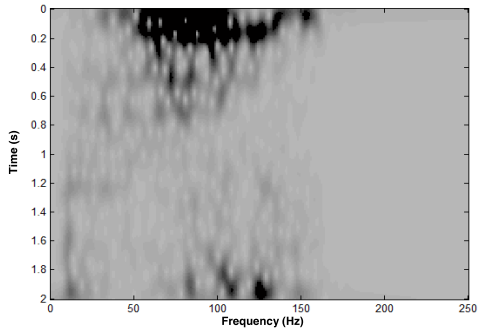

Figure 4.9. Magnitude of the Gabor transform of the estimated reflectivity by the Wiener spiking deconvolution in Figure 4.6.

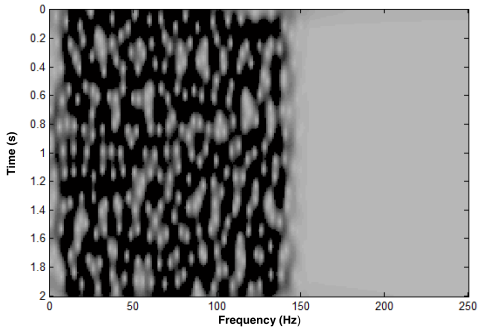

Figure 4.10. Magnitude of the Gabor transform of estimated reflectivity by Gabor deconvolution in Figure 4.6.

IV. COLOR CORRECTION FOR GABOR DECONVOLUTION

4.1 Theory of the color correction method

If the assumption of white reflectivity is violated, i.e. deviates from unity significantly, which is usually true in practice. Then deconvolution algorithm discussed above should modify accordingly, since it always gives estimation result with white amplitude spectrum ( ), which may differ from the true nonwhite reflectivity apparently. If some relevant regional well log information is available, we can conduct color correction to the Gabor deconvolution. Suppose that is the Gabor transform of the nonwhite reflectivity calculated from a well log, and is the corresponding smoothed amplitude spectrum. The Gabor deconvolution operator with color correction can be formulated as (Cheng and Margrave, 2009a) where is the stability factor, is the maximum value of is given by the Hilbert transform (over frequency),

$$D_c(\tau,f)=\frac{|R'_G(\tau,f)|}{|S_G(\tau,f)|+\mu A_{max}}e^{j\varphi_c(\tau,f)},$$

(4.23) what we need is only a smoothed Gabor amplitude spectrum. Neither detail nor phase information is needed. It is quite likely that this required well information is a very slowly changing function of position so that wells that are quite distant can still be used for color correction to conventional Gabor deconvolution. The estimated result with the white reflectivity assumption can be viewed as a special case where is nearly constant. When the real has obvious amplitude fluctuations, a white-reflectivity estimation tends to enlarge some particular parts of reflectivity series, which correspond to the low amplitude areas of . In addition, the effect of color correction depends on how much departs from unity or a constant and how reliable the employed is, which, in turn, is subject to the available frequency band and completeness of well log information. The key point of the correction method is that how to obtain an appropriate . If sufficient well log information is available, and nearly have the same length in time, which can be denoted by a time interval . can be directly obtained from the Gabor spectrum of . For this case, color correction can improve the reflectivity estimation effectively.

V. PRACTICAL CONSIDERATIONS FOR THE COLOR CORRECTION METHOD

In practice, the well log is usually incomplete and limited to some depth range, which corresponds to only a part of the whole seismic trace recorded at the surface. On this occasion, we need to use the limited well log to estimate a complete , which should be of the same size with in time-frequency domain as indicated by equation (4.25). There may be different ways to achieve this. One way assumes that the color feature of nonwhite reflectivity is temporally stationary, i.e. only changes with frequency . Suppose that is the incomplete reflectivity series with a time interval ( ), and its' Fourier spectrum is

$$|\acute{R}_c(f)|\approx a_0+a_1f+a_2f^2$$

, (4.26) where , and are constants determined using a least-squares algorithm. So, can be modeled as

International Journal of Recent Development in Engineering and Technology
Website: www.ijrdet.com (ISSN 2347 - 6435 (Online)) Volume 2, Issue 2, February 2014)

$\overline{|R'_G(\tau,f)|} = a_0 + a_1 f + a_2 f^2$. (4.27) As an alternative, another way derives the incomplete reflectivity , based on an assumption that the color feature of nonwhite reflectivity is slowly time-variant.

First, is smoothed. When multiple well logs of the same region are available, we can take full advantage of all available information. First, the Gabor spectra of well-log reflectivities are smoothed using equation (4.28). So, we can get a set of coefficient curves. Then, is still modeled by equation (4.29), while is calculated by combining all the coefficient curves of each well log through interpolation and extrapolation. Through this approach, we can approximate the true very well if the well logs are well distributed in time and the color feature of nonwhite reflectivity is not drastically time-variant.

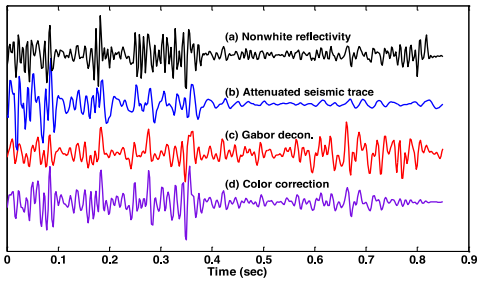

Figure 4.14. Gabor deconvolution with a frequency band of $10Hz - 100Hz$. (a) Nonwhite reflectivity. (b) Synthetic attenuated trace. (c) Gabor deconvolved trace without color correction. (d) Gabor deconvolved trace with color correction using a complete reference well log.

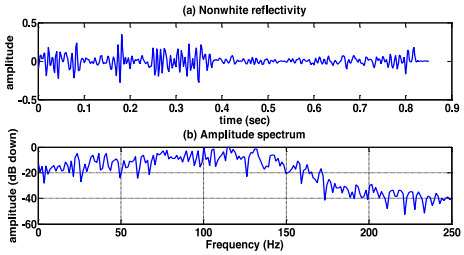

Figure 4.11. (a) Nonwhite reflectivity calculated from well log 14-09. (b) The amplitude Fourier spectrum of nonwhite reflectivity.

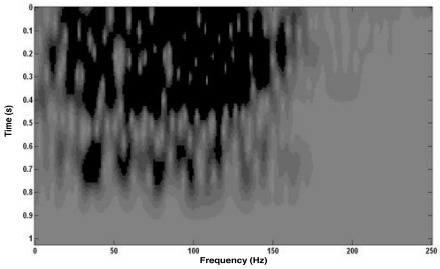

Figure 4.12. Amplitude Gabor spectrum of the nonwhite reflectivity shown in Figure 4.11.

Application of the color correction method to field data

The field data used to test our color correction method is a 2D seismic line with 159 shots and 151 receiver stations, which was acquired over Blackfoot field near Strathmore, Alberta in 1995. The reference well log is well 14-09 with a recorded depth range from to about , and which is about away from the seismic line and can be projected to the seismic line using the X-Y coordinates.

The spectral color correction is probably more of our interest from the point view of deconvolution due to its connection with phase rotation of the estimation result. The spectral color can be regarded as normalized color correction. Since the spectral color is not sensitive to the alignment error of well log to field data, spectral color correction may be preferable for prestack deconvolution. The spectral and temporal color correction can be a choice for poststack deconvolution. For spectral color correction case, both prestack and poststack deconvolution was conducted using Gabor deconvolution with spectral color correction. For the full color correction case, Gabor deconvolution with spectral color correction and Gabor deconvolution with full color correction were used for prestack deconvolution and poststack deconvolution respectively.

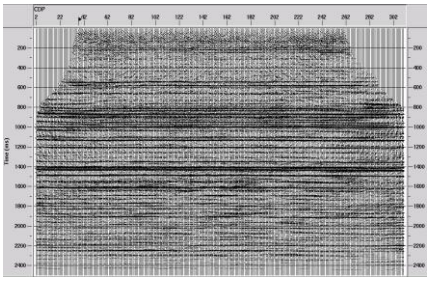

Figure 4.37. Migrated seismic data with spectral color correction applied.

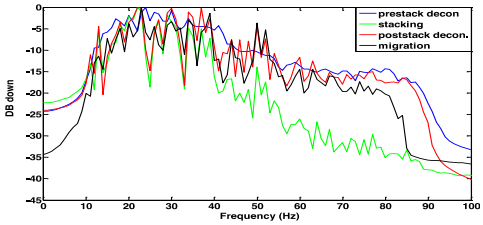

Figure 4.43. The average amplitude spectral of seismic data at different stage of data processing flow for the spectral color correction case. Blue: after prestack decon. (FFID: 7, CHAN 21-71, time: $800ms - 1800ms$); Green: after stacking (CDP 150-200, time: $500ms - 1500ms$); Red: after poststack decon. (CDP 150-200, time: $500ms - 1500ms$); Black: after Kirchhoff time migration (CDP 150-200, time: $500ms - 1500ms$).

International Journal of Recent Development in Engineering and Technology
Website: www.ijrdet.com (ISSN 2347 - 6435 (Online)) Volume 2, Issue 2, February 2014)

The phase rotation for the spectral color correction case and full color correction case is similar and comparable to the conventional Gabor deconvolution case. So, with color correction applied, seismic data has more high frequency components and roughly tie better to the well log data. In other words, color correction can improve the resolution of seismic data.

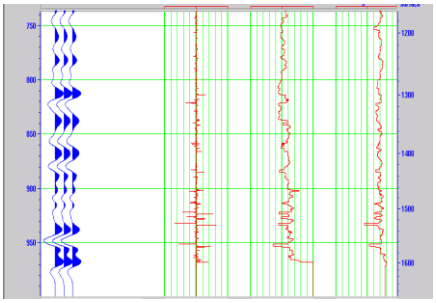

Figure 4.44. Lower part the well 14-09. From left to right: synthetic seismic trace, computed reflectivity, P wave velocity and density.

VI. CONCLUSION

The Gabor transform decomposes a signal into time-frequency domain by windowing the signal with a set of windows and then doing the Fourier transform, which provide a local spectrum of a signal. By this localization processing, Gabor transform can extend the Fourier transform to the nonstationary realm. The discrete Gabor transform can be easily realized using an approximate way, whose error can be well controlled by properly choosing of parameters. The Gabor deconvolution algorithm is developed based on a nonstationary convolution model. It can estimate the attenuated propagating wavelet, which can address the constant- attenuation inherently and is equivalent to applying an inverse- compensation to seismic trace when conducting the deconvolution. Therefore, Gabor deconvolution can be regarded as a combination of stationary deconvolution, inverse- filtering and gain correction. Testing on synthetic data shows that Gabor deconvolution can provide better estimation of reflectivity than conventional Wiener spiking deconvolution.

Reference

[1] Aki, K., and Richard, P. G., 1980, Quantitative Seismology, W. H. Freeman and Co.,San Fransisco.
[2] Banik .N. C., Lerche, I., and Shuey, R. T., 1985, Stratigraphic filtering, Part 1: Derivation of the O'Doherty- Anstey formula: Geophysics, 50: 2768 – 2774.
[3] Bath, M., 1974, Spectral analysis in geophysics: Developments in Solid Earth Geophysics, Vol 7, and Elsevier Science Publishing Co.
[4] Blanch, J. O., Robertsson, J. O. A., and Symes, W. W., 1993, Viscoelastic finite-difference modeling: Tech. Rep, 93-04, Department of Computational and Applied Mathematics, Rice University.
[5] Cheng, P., and Margrave, G. F., 2011c, Color correction for Gabor deconvolution: a test with field data: 2011 CSPG CSEG CWLS convention, abstract.
[6] Christensen, R. M., 1982, Theory of viscoelasticity – An introduction: Academic Press, Inc. Clark, G. K. C., 1968, Time-varying deconvolution filters: Geophysics, 33, 936-944.
[7] Dasgupta, R., and Clark, R. A., 1998, Estimation of from surface seismic reflection data: Geophysics, 63, 2120-2128.
[8] Engelhard, L., 1996, Determination of the seismic wave attenuation by complex trace analysis: Geophysical Journal International, 125, 608-622.
[9] Frazer, L. N., 1978, Synthesis of shear-coupled PL: Ph.D thesis, Princeton University.
[10] Frazer, L. N., and Gettrust, J. F., 1984, On a generalization of Filon's method and the computation of oscillatory integrals of seismology: Geophys. J. Roy. Astr. Soc., 72, 193-211.
[11] Griffiths, L. J., F. R. Smolka, and L. D. Trembly, 1977, Adaptive deconvolution: A new technique for processing time-varying seismic data: Geophysics, 42, 742-759.
[12] Hackert, C. L., and Parra, J. O., 2004, Improving estimates from seismic reflection data using well-log-based localized spectral correction: Geophysics, 69, 1521-1529.
[13] Kennett, B. L. N., 1975, the effect of attenuation on seismograms: Bull. Seis. Soc. of Am., 43, 17-34.
[14] Margrave, G. F., M. P. Lamoureux, and D. C. Henley, 2011, Gabor deconvolution: Estimating reflectivity by nonstationary deconvolution of seismic data: Geophysics, 76, W15- W30.
[15] Murchy, W. F. III, 1982, Effects of partial saturation on attenuation in Massilon sandstone and Vycor porous glass: J. Acoust. Soc. Am., 71, 1458-1468.
[16] Pratt, R. G., and Worthington, M. H., 1990, Inversion theory applied to multisource crosshole tomography. Part I: Acoustic wave-equation method: Geophys. Prosp., 38, 287-310.
[17] Quan, Y., and Harris, J. M., 1997, Seismic attenuation tomography using the frequency shift method: Geophysics, 62, 895-905.
[18] Raikes, S. A., and R. E. White, 1984, Measurements of earth attenuation from downhole and surface seismic recordings: Geophysical Prospecting, 32, 892-919.
[19] Robertsson, J. O. A., Blanch, J. O., and Symes, W. W., 1994, Viscoelastic finite-difference modeling: Geophysics, 59, 1444-1456.
[20] EOS, Trans., Am. Geophys. Union, 59, 324.
[21] Slepian, D., 1978, Prolate spheroidal wave function, Fourier analysis, and uncertainty – V: The Discrete case: Bell Syst. Tech. J., 57, 1371- 1429.
[22] Song, S., and K. A.Innanen, 2002, Multiresolution modeling and wavefield reconstruction in attenuating media: Geophysics, 67, 1192–1201.
[23] Spudich, P., and Ascher, U., 1983, Calculation of complete theoretical seismograms in vertically varying media using collocation methods: Geophys. J. Roy. Astr. Soc., 75, 101-24.
[24] Strick, E., 1967, the determination of , dynamic viscosity and creep curves from wave propagation measurements: Geophys. J. Roy. Astron. Soc., 13, 197-218.
[25] Sun, X., X. Tang, C. H. Cheng, and L. N. Frazer, 2000, P- and S-wave attenuation logs from monopole sonic data: Geophysics, 65, 755-765.

[26] Tal-Ezer, H., Carcione, J. M., and Kosloff, D., 1990, an accurate and efficient scheme for wave propagation in a linear viscoelastic medium: Geophysics, 55, 1366-1379.
[27] Thomson, D. J., 1982, Spectrum estimation and harmonic analysis: Proc. IEEE, 70, 1055-1096.
[28] Tonn, R., 1991, the determination of seismic quality factor from VSP data: A comparison of different computational methods: Geophys. Prosp., 39, 1-27.
[29] White, R. E., 1992, the accuracy of estimating from seismic data: Geophysics, 57, 1508-1511.
[30] Xu, T., and McMechan, G. A., 1995, Composite memeory variables for viscoelastic synthetic seismograms: Geophys. J. Int., 121, 634-639.